Measurement of coherent J/ψ production in ultraperipheral Pb+Pb collisions at 5.36 TeV with the ATLAS detector

Paweł Rybczyński

AGH University of Kraków

05.06.2025

Outline

- Vector meson photoproduction studies at HERA.
- Photonuclear vector meson production on nuclei.
- Physics of ultraperipheral collisions (UPC).
- Recent measurement of the exclusive J/ψ cross-section in UPC.
- Coinciding UPC processes.

LO cross-section for J/ψ photoproduction on proton

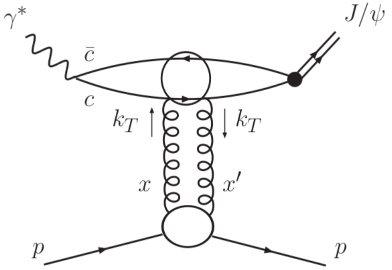

[1]

- powerful probe of the gluon distribution (at leading order),
- virtuality is assumed to be divided equally between gluons,
- VM mass provides a hard scale $\bar{Q}^2 = (Q^2 + M^2_{J/\psi})/4$, which allows use of perturbative QCD.
- $x = (Q^2 + M^2_{J/\psi})/(Q^2 + W^2_{\gamma p})$

$$\left.\frac{d\sigma}{dt}\right|_{t=0} = \frac{\Gamma_{\ell\ell} M^3_{J/\psi} \pi^3}{48\alpha} \left[\frac{\alpha_S(\bar{Q}^2)}{\bar{Q}^4} xg(x, \bar{Q}^2)^2 \left(\frac{1 + Q^2}{M^2_{J/\psi}} \right) \right]$$

The cross-section dependence on t is can be parametrized at low t as:

$$\sigma(t) \sim e^{-B(W_{\gamma p})t}$$

J/ψ meson p_{T} spectrum

The standard $xg(x, \bar{Q}^2)$ gluon PDF has the transverse distributions integrated out.

The cross-section $\sigma(\gamma p \to J/\psi p)$ can be factorized into $d\sigma/dt|_{t=0}$, which encodes all the hadronic physics of the reaction, and a form factor $F(x,t)$, which regulates the p_{T} spectrum [2]:

$$\sigma(\gamma p \to J/\psi p) = \left.\frac{d\sigma}{dt}\right|_{t=0} \int_{t_{min}}^{\infty} F(x,t)\, dt$$

where $t_{min} = M_V/2k$.

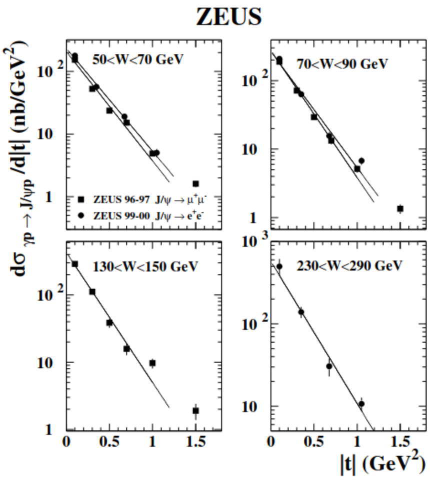

[3]

Parametrization of J/ψ

HERA measurements of J/ψ production showed a cross-section dependence on $W_{\gamma p}$ of the type [3]:

$$\sigma(\gamma p \rightarrow J/\psi p) \propto W_{\gamma p}^{\delta}$$

where $\delta = 0.69$.

The $W_{\gamma p} = 250$ GeV corresponds to $x \sim 10^{-4}$.

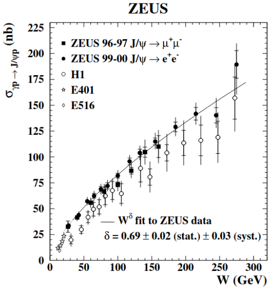

[3]

- σ increase with $W_{\gamma p}$ → influence of increasing gluon densities
- σ can't grow indefinitely → black disk regime (BDR) predicted.

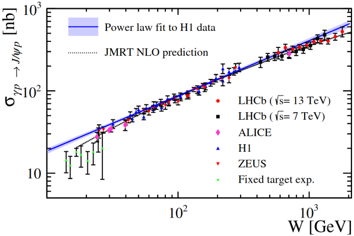

[4]

Nuclear targets

The structure of a nucleus differs significantly from a single nucleon. This can be clearly seen by looking at the nuclear modification factor $R^A_{F_2}$.

$$R^A_{F_2} = \frac{F^A_2(x, Q^2)}{A\, F^N_2(x, Q^2)}$$

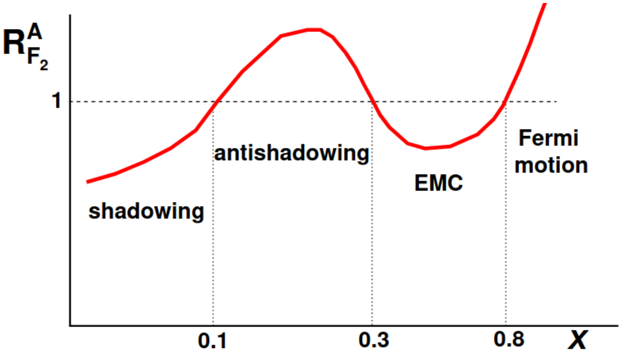

[5]

Nuclear targets

Common explanation are multiple scatterings, but the interaction mechanisms and phenomenological details vary between models [5, 6]:

- $q\bar{q}$ dipole interactions,
- Vector meson dominance,
- High density QCD (saturation physics),
- Glauber-like rescattering,
- Gribov inelastic shadowing.

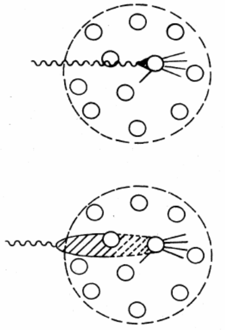

[7]

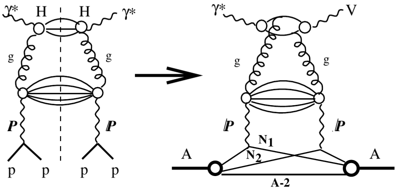

[6]

Formalism for interactions with nuclei

Vector meson production on nuclei can provide insight into it's structure, and interaction mechanism.

Ignoring the shadowing, the $\gamma A \to J/\psi A$ cross-section can be expressed using the $\gamma p \to J/\psi p$ cross-section using the Glauber calculation [2, 6]:

$$\frac{\sigma(\gamma A \to J/\psi A)}{dt} = \left.\frac{\sigma(\gamma p \to J/\psi p)}{dt}\right|_{t=0} \left| \int d^2 b \int dz \; e^{i(\vec{q_t} \cdot \vec{b} + q_l z)} \rho(b, z) e^{-\frac{1}{2}\sigma_{tot}(J/\psi p) T_A(b,z)} \right|^2$$

where $e^{i(\vec{q_t} \cdot \vec{b} + q_l z)}$ accounts for coherence across the nucleus, $\rho(b, z)$ is the nuclear density, and $T_A = \int_z^\infty \rho(\vec{b}, z') dz'$ is the nuclear thickness function.

Glauber model

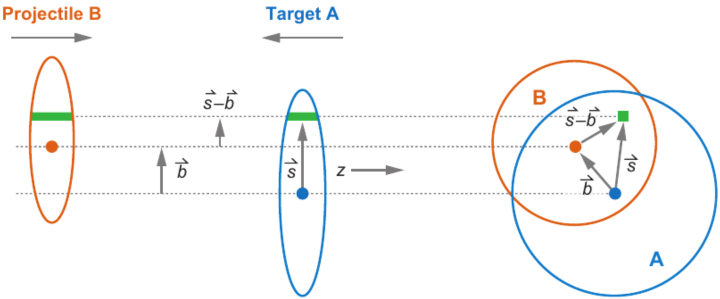

[8]

The last $e^{-\frac{1}{2}\sigma_{tot}(J/\psi p)T_A(b,z)}$ term corresponds to interaction probability along a tube in a target with given density profile.

- Different shadowing models can use modified cross-section in place of σ_{tot} (e.g. Glauber-Gribov)

Ultraperipheral collisions

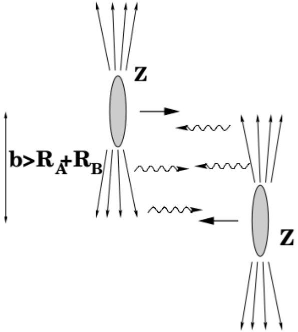

[9]

- hadronic interactions strongly suppressed,
- impact parameter $b > 2R$,
- source of quasi-real photons ($Q^2 < (\hbar/R_A)^2$),
- photon flux $N(k) \sim Z^2$.

$$\sigma(AA \to AA\, J/\psi) = \int dk \frac{dN_\gamma(k)}{dk} \sigma(\gamma A \to J/\psi\, A)$$

STARlight

One of the models available for simulation of photonuclear vector meson production events in ultraperipheral heavy-ion collisions is STARlight, which [9, 10]:

- uses the classical Glauber calculation for $\left.\frac{\sigma(\gamma A \to J/\psi A)}{dt}\right|_{t=0}$, parametrized from HERA,
- models the p_T distribution through a nuclear form factor $F(t)$,
- nuclear form factor is assumed to follow a Woods-Saxon distribution,
- uses a photon flux $\frac{dN_\gamma(k)}{dk}$ from the Weizsäcker-Williams approximation,
- assumes vector meson dominance for incoherent interactions.

$$\sigma(AA \to AA\, J/\psi) = \int_0^\infty dk \frac{dN_\gamma(k)}{dk} \left.\frac{\sigma(\gamma A \to J/\psi A)}{dt}\right|_{t=0} \int_{-t_{min}}^\infty dt\, |F(t)|^2$$

Color glass condensate

Another model [11, 12] taken into account uses the dipole picture, with the scattering amplitude:

$$-i\tilde{\mathcal{A}}(y, \mathbf{b}) = \int d^2\mathbf{r} \int_0^1 \frac{dz}{4\pi} \left[\Psi_V^* \Psi_\gamma\right](Q^2, \mathbf{r}, z) \times N(\mathbf{r}, \mathbf{b}, z, x_{\mathbb{P}}) \qquad (1)$$

where z is the fraction of the photon light-cone momentum carried by the quark, $\mathbf{r}$ the size and orientation of the dipole, Ψ_V the vector meson wave function (Boosted Gaussian), Ψ_γ the photon light front wave function.

$N(\mathbf{r}, \mathbf{b}, z, x_{\mathbb{P}})$ is the dipole-target scattering amplitude, which is described using the color glass condensate (CGC) framework:

$$N(\mathbf{r}, \mathbf{b}, z, x_{\mathbb{P}}) = 1 - \frac{1}{N_c} tr\left[V(\mathbf{b} + (1-z)\mathbf{r}) V^\dagger(\mathbf{b} - z\mathbf{r})\right] \qquad (2)$$

where the target structure is described in terms of Wilson lines $V(\mathbf{x})$.

Color glass condensate

In this model [11, 12]:

- photon p_{T} is accounted for (significant near diffractive minima),
- color charge density is assumed to be a local Gaussian variable (IPsat parametrization fitted to HERA data),
- local saturation scale is proportional to the local transverse density $Q_s^2(\mathbf{x}) \propto T_p(\mathbf{x})$,
- nucleon positions are sampled from Woods-Saxon distribution and summed toghether for the total density,
- nucleon hot-spots can also be randomly sampled from a Gaussian distribution,
- Wilson lines are obtained at $x_{\mathbb{P}} = 0.01$,
- energy dependence is obtained by solving the JIMWLK evolution equations.

J/ψ kinematics in UPC events

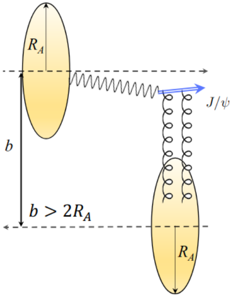

[13]

In UPC vector meson production the photon k and Pomeron q energy follow the relationship [9]:

$$k_{1,2} = \frac{M_{J/\psi}}{2} e^{\pm y}, \qquad q_{1,2} = \frac{M_{J/\psi}}{2} e^{\mp y}$$

depending on which nucleus is the photon emiter.

The Bojrken-x probed in this collisions is:

$$x = \frac{M_{J/\psi}}{\sqrt{s_{NN}}} e^{\pm y}$$

Mid-rapidity measurements of J/ψ in $|y| < 2.5$ correspond to:

$$x \sim 4.7 \cdot 10^{-5} - 5.8 \cdot 10^{-4}, \quad \text{or} \quad x \sim 5.8 \cdot 10^{-4} - 7 \cdot 10^{-3}$$

Bjorken-x ambiguity

This ambiguity can be resolved by considering J/ψ production accompanied by forward neutron emission, that can be registered by zero degree calorimeters (ZDC) [14]:

$$d\sigma^{0nXn}/dy = N_{\gamma}^{0nXn}(\omega_1)\sigma_{\gamma A\to J/\psi\ A}(\omega_1) + N_{\gamma}^{0nXn}(\omega_2)\sigma_{\gamma A\to J/\psi\ A}(\omega_2)$$
$$d\sigma^{XnXn}/dy = N_{\gamma}^{XnXn}(\omega_1)\sigma_{\gamma A\to J/\psi\ A}(\omega_1) + N_{\gamma}^{XnXn}(\omega_2)\sigma_{\gamma A\to J/\psi\ A}(\omega_2)$$

where $0nXn$ corresponds to neutron activity in one ZDC arm, and no activity in the other, and $XnXn$ to neutron activity in both ZDC arms.

J/ψ measurement

Motivation

- Filling the gap in measurements for $0.8 < y < 1.6$.
- Process sensitive to nuclear gluon dynamics at low-x.

[15]

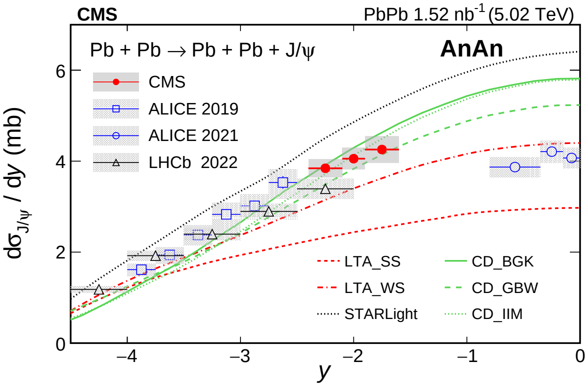

The measurement is performed in 5 J/ψ rapidity intervals: $|y| < 0.5$, $0.5 < |y| < 1$, $1 < |y| < 1.5$, $1.5 < |y| < 2$, $2 < |y| < 2.5$.

ATLAS detector

- Inner Detector coverage: $|\eta| < 2.5$, $p_{\mathrm{T}} > 0.1$ GeV.
- Calorimeter coverage: $|\eta| < 4.9$.
- Muon trigger/identification $p_{\mathrm{T}} > 4$ GeV.

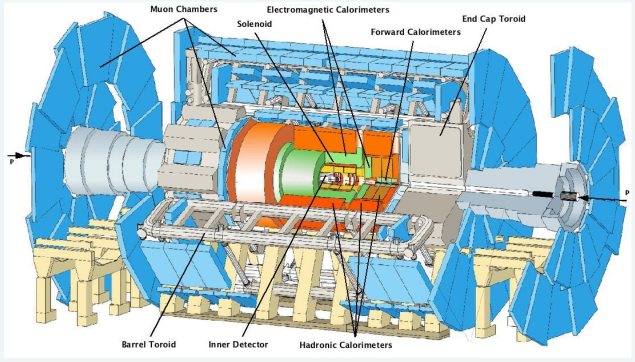

TRT Fast-OR trigger

- TRT high threshold (HT) hits used for triggering instead of electron identification.
- High threshold lowered so that any MIP produces HT hits.
- Allows to trigger directly on low-p_{T} tracks.

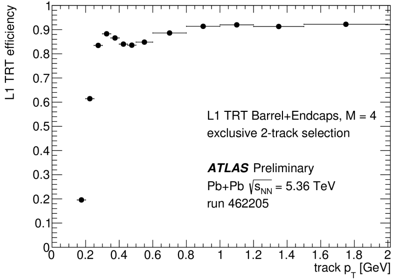

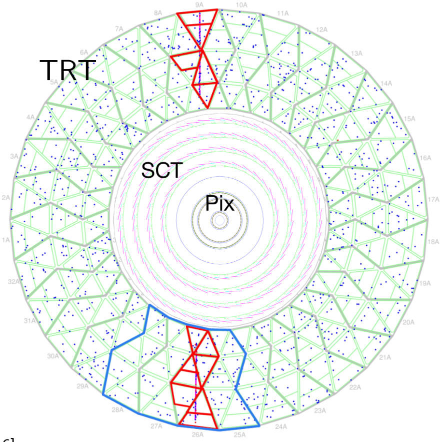

[16]

Data and simulation

Data from **2023 heavy-ion run** are used ⇒ **76.5 μb^{-1} integrated luminosity.** Data is compared to Monte Carlo samples generated by STARlight and interfaced with Pythia8 for QED FSR.

Trigger selection:

L1:

- TRT trigger signal,
- total calo $E_\mathrm{T} < 20$ GeV.

HLT:

- FCal $E_\mathrm{T} < 5$ GeV,
- 1-5 tracks with $p_\mathrm{T} > 1$ GeV,
- < 15 tracks with $p_\mathrm{T} > 0.2$ GeV.

Event selection:

- exactly 2 OS tracks with $p_\mathrm{T} > 1$ GeV, $|\eta| < 2.5$ and $|d_0| < 2$ mm and passing loose track quality selection,
- within signal region: 2.9 GeV $< m^{pair} < 3.2$ GeV and $p_\mathrm{T}^{pair} < 0.2$ GeV.

Fits to 2–track system invariant mass

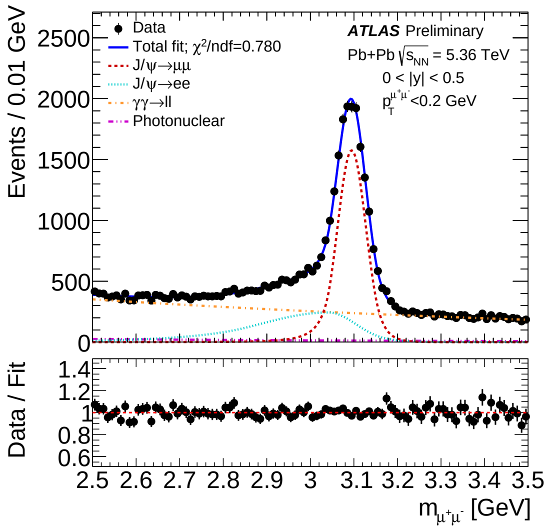

- Dilepton continuum modeled with exponential function.
- J/ψ modeled with Crystal Ball functions.
- **Shapes** are fixed from **fits to MC** simulated samples.
- In **fit to data** only the **normalizations** are allowed to change + the slope of the $\gamma\gamma \to \ell\ell$ exponent.

Photonuclear background

Photonuclear combinatorics modeled by data-driven “same-sign” templates, which are normalized to data in low-mass sideband region at high system pT.

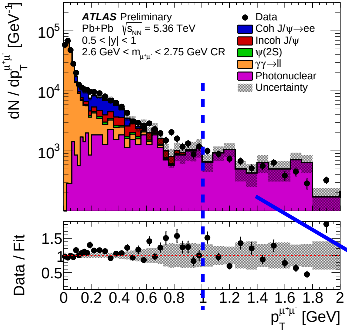

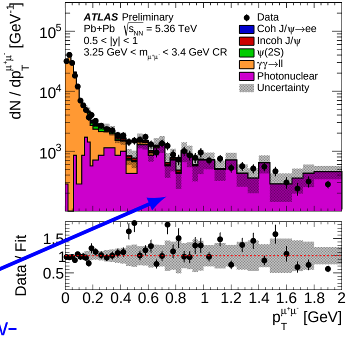

Normalization taken from low-mass sideband.

p_T fits

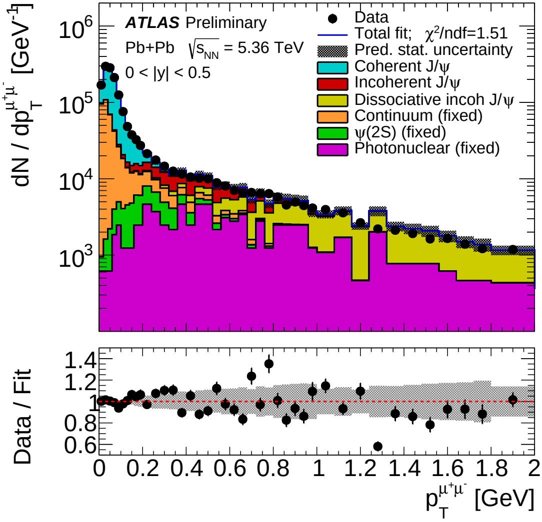

- The coherent contribution to exclusive $J/\psi \to \mu\mu$ yield is extracted from fits to the p_T distribution (in **2.9 - 3.2 GeV** track system invariant mass region).
- In the fit, the: dilepton continuum, $\psi(2S)$, and photonuclear combinatorial background templates are kept fixed.
- Dissociative incoherent contribution is parametrized (from HERA) with: $\frac{dN}{dp_T} \sim 4 b_{pd} p_T^2 (1 + \frac{b_{pd}}{n_n} p_T^2)^{(-n_n+1)}$

Systematic uncertainties

L1 TRT trigger efficiency (SFs variations, both stat. and sys.)

- **1.5-1.9%** (stat) except last bin (∼7%)
- **1-2%** (sys) except last bin (∼3.5%)

Signal and background modeling

- Signal p_{T} shape variation (p_{T} shape reweighting) → **0.3-1.6%**
- Dilepton continuum modeling (pol2 instead of expo) → **0.1-0.2%**, except last bin (∼4%)
- Mass fit methodology (difference between the nominal and alternative analyses)→ up to **3.7%**
- Incoherent background modeling → varied p_{T} fit ranges (0-2 GeV - default, 0-1 GeV + 0-3 GeV as variations) → ∼**0.2%**, except last bin (∼2%)
- 20% flat uncertainty on $\psi(2S)$ feed-down → ∼**0.5%** track veto (4 tracks allowed) → **2%**

Detector material modeling → **0.8-2.1%**
Other sources:

- $J/\psi \to \mu\mu$ branching ratio → **0.5%**
- Integrated luminosity → **3.5%**

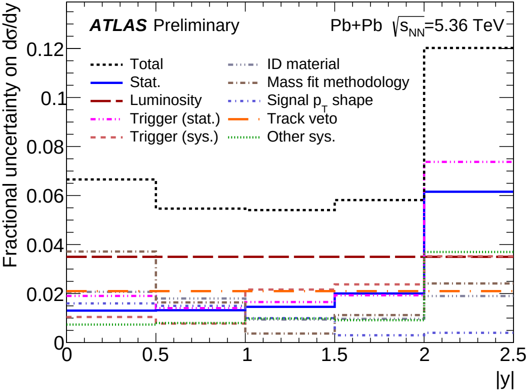

Absolute rapidity interval	0–0.5	0.5–1	1–1.5	1.5–2	2–2.5
$J/\psi \to \mu^+\mu^-$ $m_{\mu^+\mu^-}$ lineshape	1.4%	1.2%	0.7%	0.7%	1.6%
$J/\psi \to e^+e^-$ $m_{\mu^+\mu^-}$ lineshape	0.7%	0.6%	0.3%	0.2%	0.1%
$p_{\mathrm{T}}^{\mu^+\mu^-}$ shape	0.1%	0.1%	0.1%	0.2%	0.3%
Total ID material unc. on signal yield	2.1%	1.8%	0.9%	1.0%	0.8%

Measured cross-sections

$$\frac{d\sigma}{dy} = \frac{N^{coh}_{J/\psi\to\mu\mu}}{A\times C\times BR\times\mathcal{L}_{int}\times\Delta y}$$

- Comparison with two models is shown.
- Both models use HERA $\gamma p \to J/\psi p$ data as input.
- In addition, the CGC model includes effects of nucleon shape fluctuations.

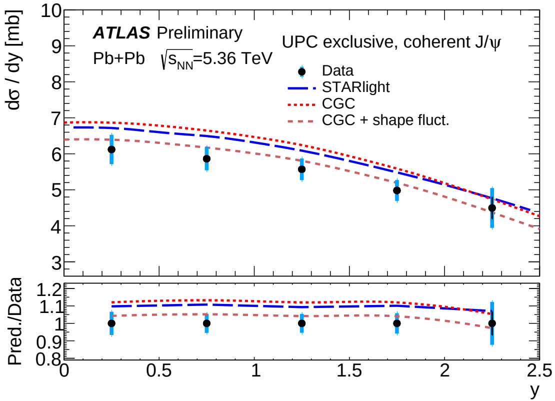

Extrapolation to 5.02 TeV

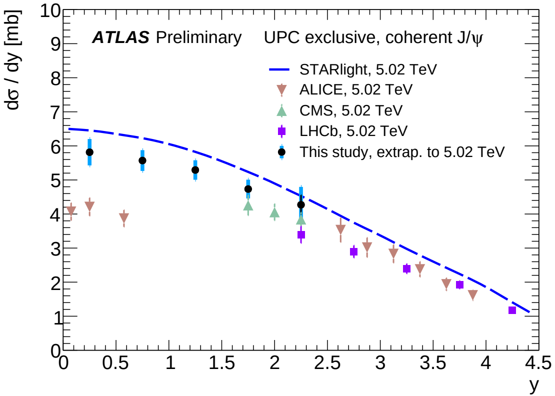

- Extrapolation of this measurements from 5.36 TeV to 5.02 TeV using STARlight predictions (about -5% correction).
- Good agreement with other experiments is observed at larger rapidities.
- Significant difference between ATLAS and ALICE at low rapidities.

ALICE measurement

- The V0 detector consists of two scintillating arrays covering the pseudorapidity ranges $2.8 < \eta < 5.1$ (V0A) and $-3.7 < \eta < -1.7$ (V0C).
- The V0 detector is used to ensure exclusivity of the process, but is sensitive to soft e^+e^- pairs from $\gamma\gamma \to e^+e^-$.

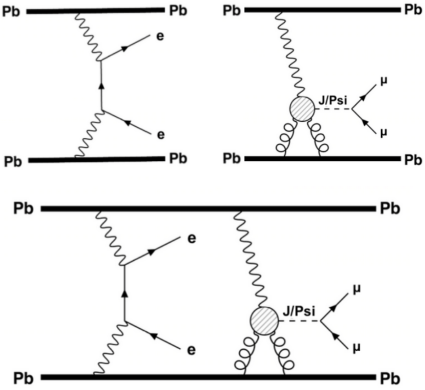

Coinciding UPC processes

Recent ATLAS measurement of dimuon photoproduction in UPC shows that for lowered impact parameter the coincidence probability increases.

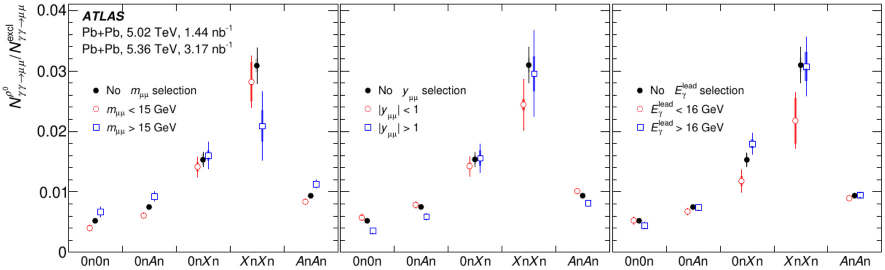

[arXiv:2504.07795]

Coinciding UPC processes

Clear $J/\psi + \rho_0$ signal is observed.

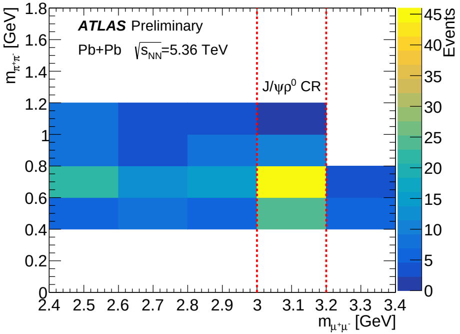

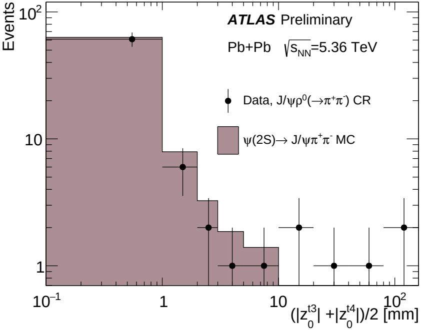

- Fraction of same to separate vertex events found to be $\sim 10:1$,
- Influence of multiple UPC processes on ALICE measurement remains unknown,
- A coincidence rate of $\sim 5:1$ could explain the difference.

Summary

1. First ATLAS measurement of coherent J/ψ production in UPC.
2. Differential cross-section measured in $|y| < 2.5$.
3. Results demonstrate a good performance of L1 TRT trigger achieved in Run 3.
4. Tension between ATLAS and ALICE observed at mid-rapidity.

Future prospects:

1. Extending the measurements to account for different ZDC activity channels.

The end

Thank you for your attention!

This work was realized as part of the NCN PRELUDIUM BIS 4 project 2022/47/O/ST2/00148

NATIONAL SCIENCE CENTRE POLAND

Bibliography I

[1] S. P. Jones et al. *Probes of the small x gluon via exclusive J/psi and Upsilon*. 2013. arXiv: 1307.7099 [hep-ph].

[2] S. R. Klein and P. Steinberg. "Photonuclear and Two-Photon Interactions at High-Energy Nuclear Colliders". In: *Annual Review of Nuclear and Particle Science* 70.1 (2020), 323–354. ISSN: 1545-4134.

[3] S. Chekanov et al. "Exclusive photoproduction of J / psi mesons at HERA". In: *Eur. Phys. J. C* 24 (2002), pp. 345–360. arXiv: hep-ex/0201043.

[4] R. Aaij et al. "Central exclusive production of J/ψ and $\psi(2S)$ mesons in pp collisions at $\sqrt{s} = 13$ TeV". In: *JHEP* 10 (2018), p. 167. arXiv: 1806.04079 [hep-ex].

[5] N. Armesto. "Nuclear shadowing". In: *Journal of Physics G: Nuclear and Particle Physics* 32.11 (2006), R367–R393. ISSN: 1361-6471.

[6] L. Frankfurt, M. Strikman, and M. Zhalov. "Fading out of J / psi color transparency in high-energy heavy ion peripheral collisions". In: *Phys. Lett. B* 540 (2002), pp. 220–226. arXiv: hep-ph/0111221.

[7] T. H. Bauer et al. "The hadronic properties of the photon in high-energy interactions". In: *Rev. Mod. Phys.* 50 (2 1978), pp. 261–436.

[8] M. L. Miller et al. "Glauber modeling in high energy nuclear collisions". In: *Ann. Rev. Nucl. Part. Sci.* 57 (2007), pp. 205–243. arXiv: nucl-ex/0701025.

[9] A BALTZ et al. "The physics of ultraperipheral collisions at the LHC". In: *Physics Reports* 458.1–3 (2008), 1–171. ISSN: 0370-1573.

[10] S. R. Klein et al. "STARlight: A Monte Carlo simulation program for ultra-peripheral collisions of relativistic ions". In: *Computer Physics Communications* 212 (2017), 258–268. ISSN: 0010-4655.

[11] H. Mäntysaari, F. Salazar, and B. Schenke. "Nuclear geometry at high energy from exclusive vector meson production". In: *Phys. Rev. D* 106.7 (2022), p. 074019. arXiv: 2207.03712 [hep-ph].

Bibliography II

[12] H. Mäntysaari, F. Salazar, and B. Schenke. "Energy dependent nuclear suppression from gluon saturation in exclusive vector meson production". In: *Phys. Rev. D* 109.7 (2024), p. L071504. arXiv: 2312.04194 [hep-ph].

[13] M. I. Abdulhamid et al. "Exclusive J/ψ, ψ(2s), and e+e− pair production in Au+Au ultraperipheral collisions at the BNL Relativistic Heavy Ion Collider". In: *Phys. Rev. C* 110.1 (2024), p. 014911. arXiv: 2311.13632 [nucl-ex].

[14] V. Guzey, M. Strikman, and M. Zhalov. "Disentangling coherent and incoherent quasielastic J/ψ photoproduction on nuclei by neutron tagging in ultraperipheral ion collisions at the LHC". In: *Eur. Phys. J. C* 74.7 (2014), p. 2942. arXiv: 1312.6486 [hep-ph].

[15] A. Tumasyan et al. "Probing Small Bjorken-x Nuclear Gluonic Structure via Coherent J/ψ Photoproduction in Ultraperipheral Pb-Pb Collisions at sNN=5.02 TeV". In: *Phys. Rev. Lett.* 131.26 (2023), p. 262301. arXiv: 2303.16984 [nucl-ex].

[16] *Performance plots*. https://atlas.web.cern.ch/Atlas/GROUPS/PHYSICS/PLOTS/IDET-2023-01/. Accessed on 03.06.2025.